Leadership in Sustainable Infrastructure

Leadership en Infrastructures Durables

Vancouver, Canada

May 31 – June 3, 2017/ *Mai 31 – Juin 3, 2017*

A DYNAMIC ANALYSIS OF A NOVEL SHAPE MEMORY ALLOY-BASED BRACING SYSTEM

Zareie, Shahin[1,5], M. Mirzai, Nadia [2], Alam, Shahria [3], and Seethaler, Rudolf J.[4]

[1]Graduate Research Assistant, EME 3204, School of Engineering, The University of British Columbia, Kelowna, BC, Canada
[2]Graduate Research Assistant, School of Civil Engineering, University of Tehran, Tehran, Iran
[3]Associate Professor, EME 4205, School of Engineering, The University of British Columbia, Kelowna, BC, Canada
[4]Associate Professor, EME 4205, School of Engineering, The University of British Columbia, Kelowna, BC, Canada
[5]shahin.zareie@ubc.ca

Abstract:

Shape memory alloys (SMAs) reveal unique characteristics including shape memory and superelastic effects which make them excellent candidates for civil infrastructure applications. They can have a great effect in preventing the structural damages which might occur during earthquake events. The smart system in which SMA is used can undergo a large amount of deformation and return to its initial shape after the removal of loading, and dissipate energy of loading. Due to the recovery capability (superelasticity) of SMA, the novel SMA-based bracing system is proposed to implement into building. It improves the dynamic behaviour of building by mitigation of seismic hazards and dissipate energy with re-entering capability in tension and compression mode during and after seismic events.

In order to examine the performance of suggested system, a 4-story steel frame is modeled with BRBF and SMA the bracing system. Dynamic analyses are conducted to investigate the effect of bracing on the response of the structure.

1.1 Introduction

Medium or severe earthquakes can lead to the occurrence of permanent damage with residual deformation in civil infrastructure. Thus, engineers should consider the effect of earthquake loads when designing infrastructure that has enough strength, damping, capacity of energy dissipation, ductility, and so on (Talebi et al. 2010). However, meeting these parameters have been expensive or impossible due to the inherent characteristics of civil structures. In order to supply them, different methods have been used such as bracing systems. But, conventional bracing systems were passive and did not dissipate the energy of strong earthquakes adequately(Talebi et al. 2014).

In the last decades, research has suggested new materials to be used in bracing systems such as shape memory alloys(SMA)(Eatherton et al. 2014). SMA is a class of material which is capable of returning to the original shape while mechanical loads are removed (superelasticity) or heat is applied to SMA (shape memory effect).In addition, SMA absorbs energy during loading and unloading phases.

Krumme et al. (Krumme et al. 1995) introduced a damper based on NiTi-SMA to withstand seismic loads. The system was implemented into a three-story steel frame. Then, a nonlinear dynamic time history analysis proved that the novel system was accurate and enhanced the dynamic behaviour. Additionally, results demonstrated that pre-tensioning SMA wires increased the amount of energy dissipation. Massah et al. (Massah & Dorvar 2014) studied eccentric bracing frame with shape memory alloy (SMA) on 4, 9 and 14 steel frames. The maximum interstory drift (ID) and the residual deformation were surprising lessen by using the bracing system. The study showed that full recovery was possible in all frames of the structure, when earthquake loads strained the SMA wires less than 6% . Gao et al. (Gao et al. 2016) discussed the analytical and experimental tests on an innovative SMA ring-shape implemented into the bracing system. The experimental tests under a quasi-static load proved a high capacity for dissipating energy and re-centering ability; it also increased the damping. Their investigation was also proposed to decrease the residual deformation of other connections by rigid cable and/or steel truss members. The experimental results demonstrated that the finite element model of this bracing was adequate and verified the design in a small interstory drift. In the proof-of-concept, the thermal effect was not considered. Thus, an extensive study was suggested to obtain better knowledge of response characteristics. Moradi et el.(Moradi et al. 2014) investigated a four-story steel frame with concentrically NiTi shape memory alloy bracing system and buckling-restrained braced frames (BRBFs) using OpenSees software. The incremental dynamic analysis for four types of bracing systems was achieved for 20 ground motion records to evaluate the performance of all systems. The effect of the bracing systems was highlighted while the intensity of ground motions (GMs) increased. Results of the pushover analysis showed that the influence of excitation frequencies in buckling-restrained braces was less than SMA braced frames (SMA-BFs).

In this study, a novel SMA bracing system is suggested to install in buildings to dissipate energy with re-entering capability during and after seismic events. In order to examine the smart system, OpenSees software is used to model and perform a time-history analysis for the proposed NiTi-based bracing system in a four-story steel frame and compared with the BRBFs.

1.2 Shape Memory Alloy (SMA)

SMA is a new class of material alloy which can recover its original shape after undergoing large deformation as a result of the superelasticity and\or the shape memory effect (SME). In order to recover the predefined state, heat must be applied to the SMA in the SME, and the external load must be removed from SMA in the superelasticity (Hedayati Dezfuli 2015). In this research, it is assumed that temperature is greater than the Austenite finish temperature; the superelasticity is thus the only characteristic considered.

There are two phases in the SMA. The first phase is the loading phase (the Austenite phase to the Martensite phase); this phase starts from the Martensite start strain (ε_{ms}) and reaches to the Martensite finish strain (ε_{mf}). The second phase is the unloading phase, which is the Martensite phase to the Austenite

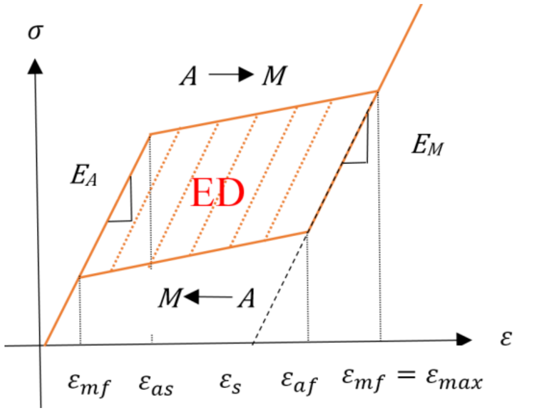

phase (as shown in

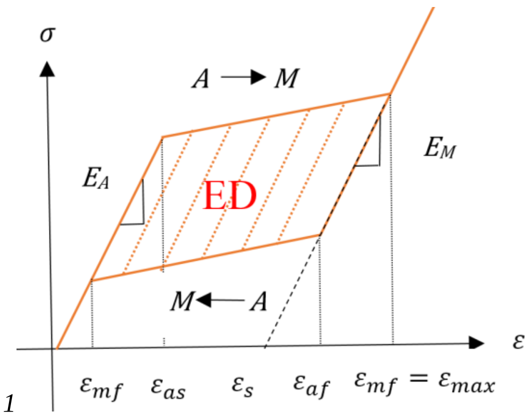

Figure *1*

Figure 1); it begins with the Austenite starts strain (ε_{as}) and ends with the Austenite finish strain (ε_{af}) (Hedayati Dezfuli 2015).

Three more important parameters are shown in Figure 1: the maximum superelastic strain(ε_s) and maximum applied strain($\varepsilon_{\max}$) which is fully recovery capability after undergoing large deformation. E_A is the elastic modulus

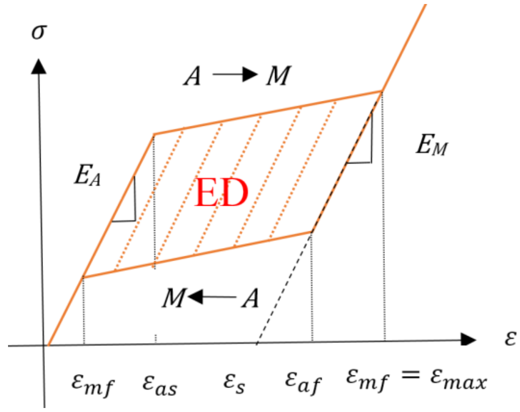

Figure 1.The strain-stress response of SMA

1.3 Material

The properties of the steel and SMA are illustrated in Table 2 and **Error! Reference source not found.**. The elastic modulus and yield stress of steel are 200 GPa and 235 MPa, respectively.

$\varepsilon_{\max}$ and ε_s are 6% and 4.6%. Another important parameter is the Austenite finish temperature (A_f), which is about 53º. The E_A is about 28 GPa.

Table 1. The mechanical properties of steel

Alloy	Density (kg/m^3)	Elastic Modulus (GPa)	Poisson's Ratio	Yield Strength (MPa)	Reference
Steel	7850	200	0.3	235.36	(Moradi et al. 2014)

Table 2. The SMA properties

Alloy	$\varepsilon_{\max}(\%)$	$\varepsilon_s(\%)$	$E_A(Gpa)$	$A_f(^o c)$	Reference
NiTi	6	4.6	28	53	(Hedayati Dezfuli & Alam 2013)

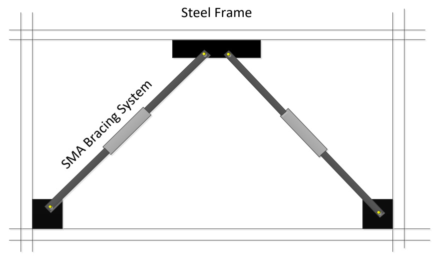

Figure 2. The schematically diagram of the inverted-V SMA bracing system

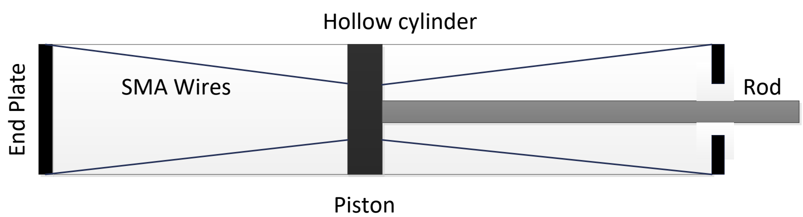

Figure 3. The schematically diagram of inverted-V

1.4 SMA bracing system

The suggested Inverted-V SMA system, which is installed in the steel frame, is shown in Figure 2. The simplified model is displayed in Figure 3. The main elements of the system are a hollow cylinder, SMA wires, a piston, an end plate, and a rod.
The operation of the system as displayed in Figure 4 is as follows: in compression mode, the right side SMA wires generate resistance force (1); in tension mode, the left side SMA wires supply force against external excitation (2). During earthquake events, earthquake loads force civil infrastructure to move to both sides; thus, the benefits are that the SMA bracing system dissipates energy of the external loads.
Table 3 illustrates the characteristics of each diagonal bracing system embedded in the inverted-V bracing system. It is composed of 100 SMA wires on each side, each 1700 mm in length.

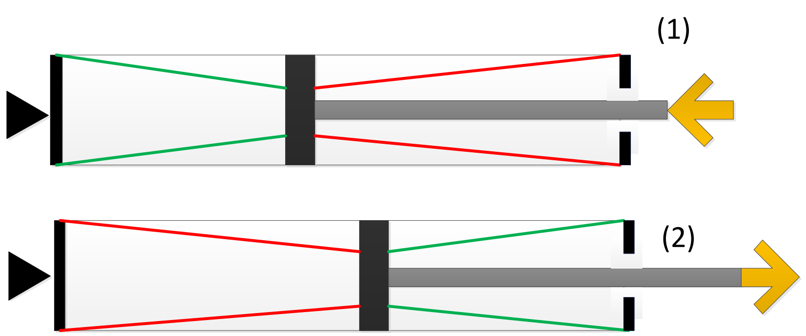

Figure 4. The operational mechanism of SMA bracing system

Table 3. The dimensions of the SMA bracing system

Bracing SMA material	Length(mm)	Radius of piston base(mm)	Thickness of Piston(mm)	Number of SMA wires	Angle(^{o})
NiTi	3410	50	10	100	15

1.5 Ground motions selection

According to Iranian code of practice for seismic resistant design of buildings (Code 2014) , the acceleration time histories, representing the ground motion effects, shall reflect the expected earthquake acceleration at the site. Furthermore, the minimum of the three pairs of appropriate horizontal ground motion components is used and scaled properly. The detail of selection and scaling of ground motions is found in Code 2014.

Three far field ground motion records are selected (as listed in Table 4) from FEMA P695 (downloaded from PEER (Pacific Earthquake Engineering Research Center)) for nonlinear time history analysis. The magnitude of all earthquakes range between 6.5 and 7.3. The soil type D is based on the US Geological Survey (USGS), which is equivalent to soil type C in Code 2014. The acceleration of ground motion records is shown in Figure 5.

Table 4. Properties of three selected ground motion

ID No.	M	Soil type1	Year	Record Name	Station Name
960	6.7	D	1994	Northridge	Canyon Country-WLC
169	6.5	D	1979	Imperial Valley	Delta
848	7.3	D	1992	Landers	Coolwater

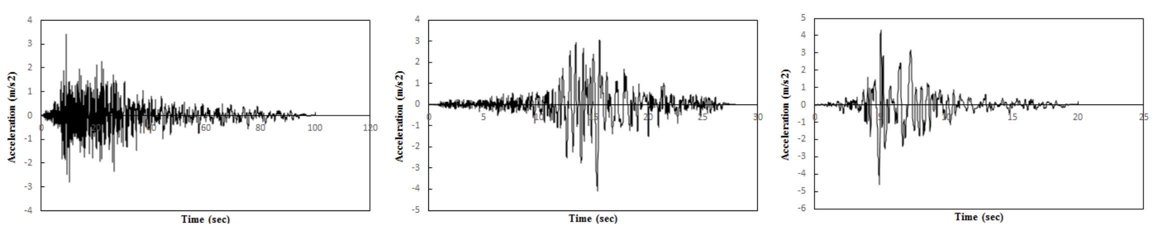

(1) (2) (3)

Figure 5. The ground motion profiles: (1). Northridge (2). Imperial Valley (3). Landers

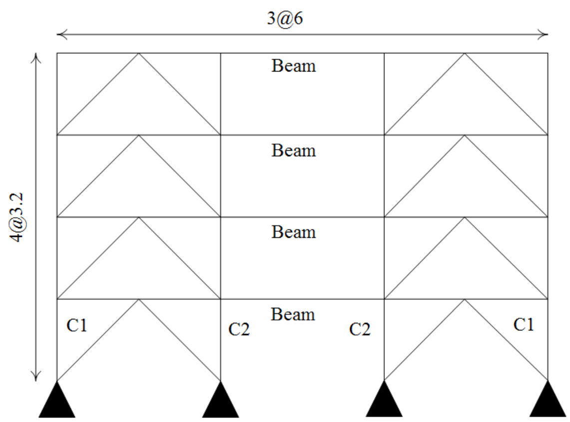

Figure 6. The schematic diagram of steel frame with inverted-V bracing systems (the main structure is adapted from (Moradi et al. 2014))

1.6 Modeling

Models for the braced frames are developed in OpenSees (the Open System for Earthquake Engineering Simulation) software as shown in Figure 6.

The beams, columns, and braces are simulated as nonlinear “beam-column fiber members”. Fibers exhibit bilinear behavior i.e. elastic-plastic stress-strain (“Steel01”) with a hardening ratio of 0.025. Figure 7. The steel 01 in Opensess schematically.

The Giuffre-Menegotto-Pinto hysteretic material (“Steel02”) is employed for modeling braces which combines the Bauschinger and isotropic hardening effect for a smooth conduction from the elastic to the hardening branch (as displayed in Figure 8).

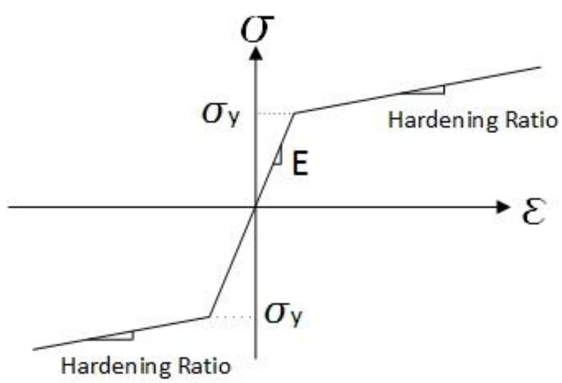

Figure 7. The steel 01 in Opensess

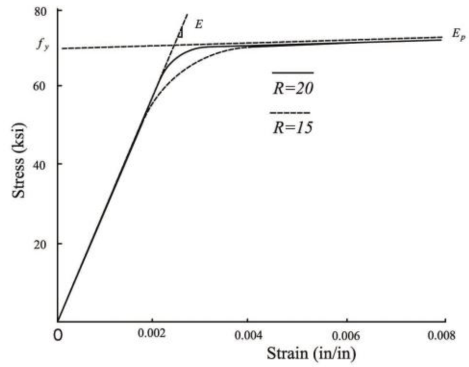

Figure 8. The steel 02 in Opensess

All beams and braces are pinned end element. For this aim, two parallel coordinate nodes are considered for the start and the end of aforementioned members (elements) and are restrained with ZeroLength element with rigid material in translational directions.

Also, the diaphragm in each floor is considered rigid by using the equalDOF command. Rayleigh damping with damping coefficient 5% is employed in the model. The dead and live loads are 6 kN/m and 2 kN/m, respectively.

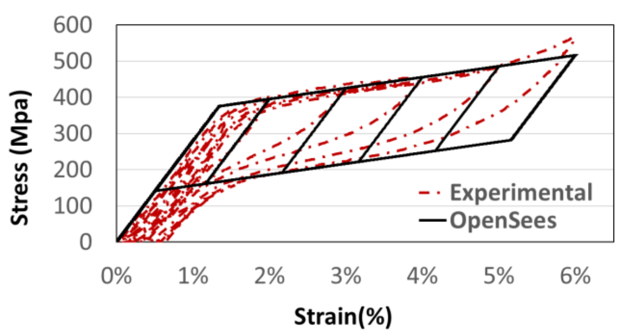

Figure 9. The comparison between hysterias of NiTi in OpenSees and experimental test

The uniaxial self-centering material is considered to model the SMA bracing system and is verified using experimental results, which were obtained by Hedayati et al. (Dezfuli & Alam 2013). Figure 9 shows the comparison between the strain-stress in OpenSess and the experimental results.

1.7 Frame specification

The SMA bracing system is examined in a steel frame, which is designed by Asgarian et al. (Moradi , et al. 2014). The steel frame with the embedded inverted-V bracing system is shown schematically in Figure 6. The length of the bay is 6 m and the height of each story is 3.2 m.

The characteristics of this frame are displayed in Table 5. IPB200 is used for C1 of the first and second floor and IPB140 is utilized for C2 of the third and fourth floor. IPE300 and IPE360 are used for the roof beam and other stories' beams.

Table 5. The model specifications of four-story steel frame with bracing system (adapted from (Moradi et al. 2014))

Bracing type / Story	Diagonal SMA Bracing system					Diagonal BRBF				
	C1	C2	Beam	Area	Bracing material	C1	C2	Beam	Area	Bracing material
1	IPB200	IPB220	IPE360	706.85	NiTi	IPB200	IPB220	IPE360	425	Steel
2	IPB200	IPB220	IPE360	615.75	NiTi	IPB200	IPB220	IPE360	375	Steel
3	IPB140	IPB160	IPE360	615.75	NiTi	IPB140	IPB160	IPE360	300	Steel
4	IPB140	IPB160	IPE300	615.75	NiTi	IPB140	IPB160	IPE300	200	Steel

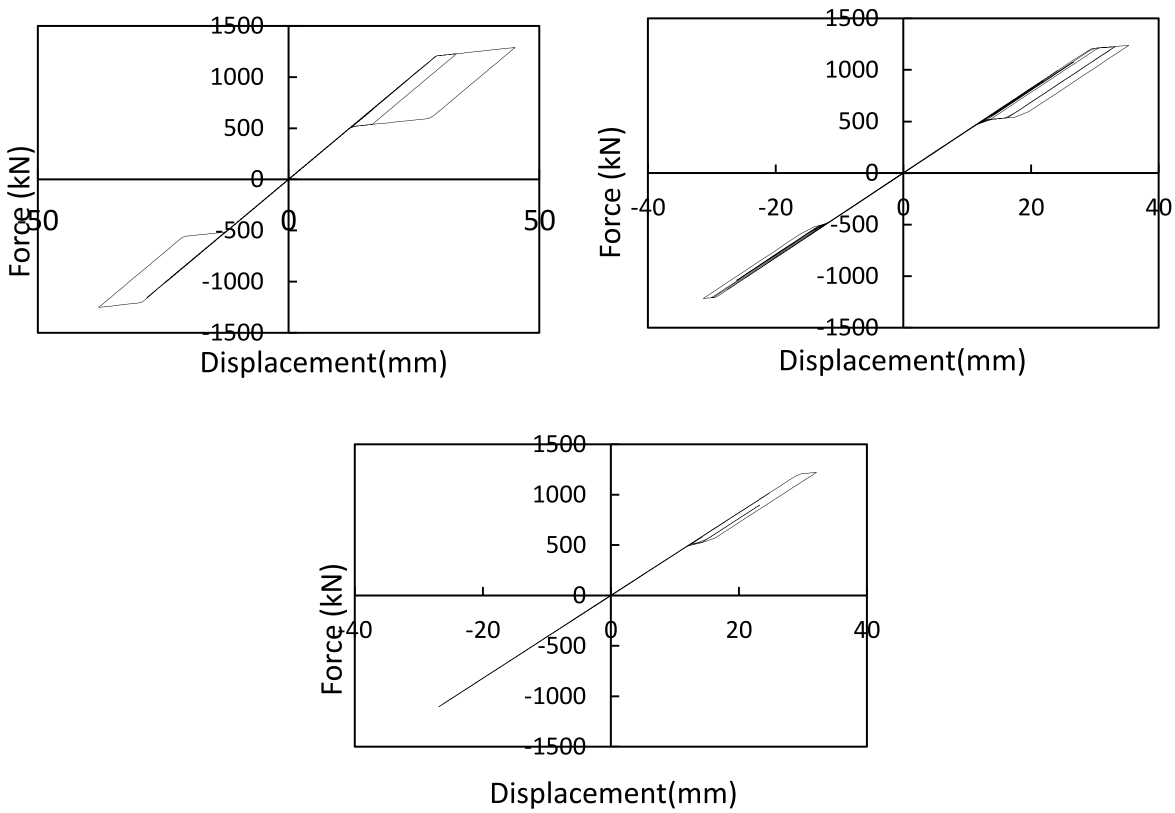

Figure 10. The force-displacement responses of SMA bracing systems under three earthquake loads

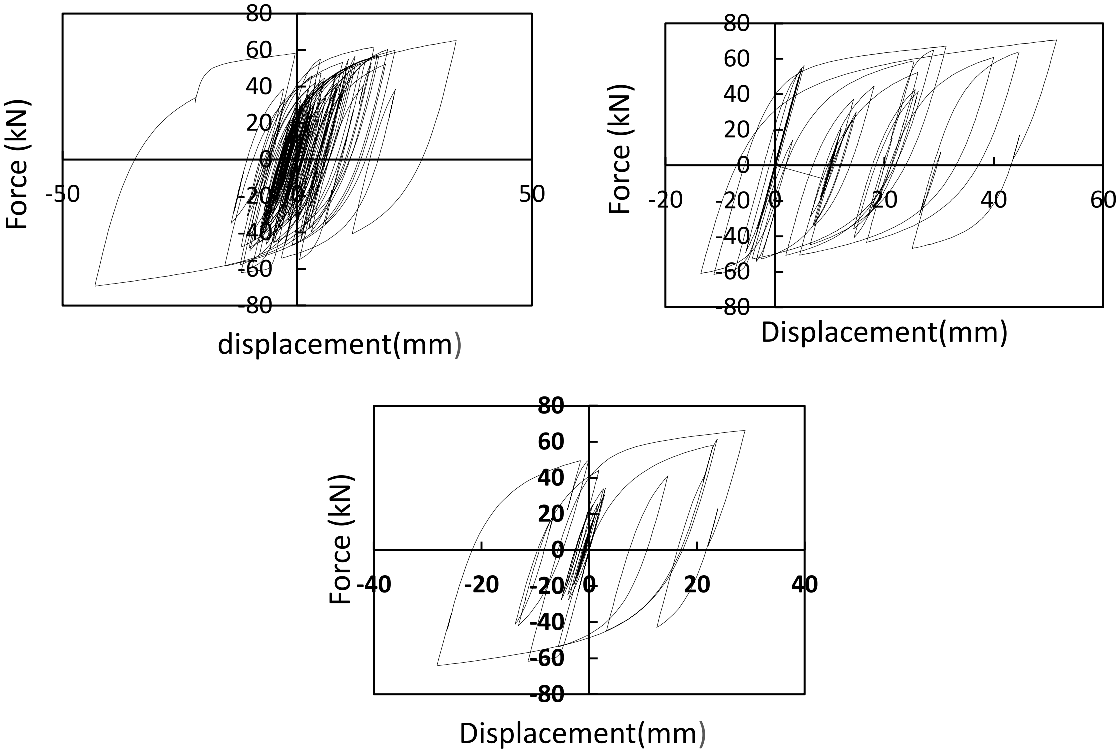

Figure 11. The force-displacement responses of BRBF under three earthquake loads

1.8 Results

In order to examine the bracing systems, the three GMs, as discussed earlier, are applied to the steel frames with the SMA bracing system and BRBF.

The hysteresis responses of the second floor of the SMA bracing system and the BRBF under all GMs are shown in

Bracing type / Story	Diagonal SMA Bracing system					Diagonal BRBF				
	C1	C2	Beam	Area	Bracing material	C1	C2	Beam	Area	Bracing material
1	IPB200	IPB220	IPE360	706.85	NiTi	IPB200	IPB220	IPE360	425	Steel
2	IPB200	IPB220	IPE360	615.75	NiTi	IPB200	IPB220	IPE360	375	Steel
3	IPB140	IPB160	IPE360	615.75	NiTi	IPB140	IPB160	IPE360	300	Steel
4	IPB140	IPB160	IPE300	615.75	NiTi	IPB140	IPB160	IPE300	200	Steel

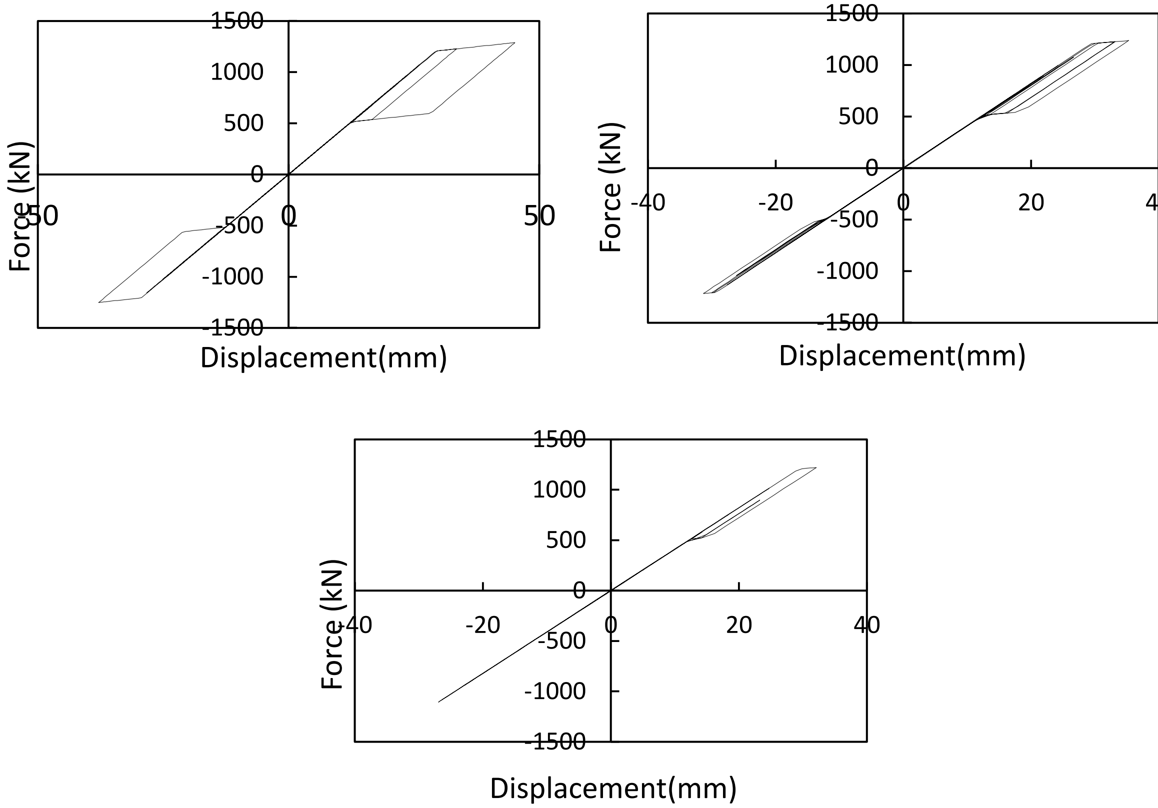

Figure 10 and in Figure 11. It is noted that the amount of energy dissipation of the BRBF is greater than the SMA bracing system in all cases. In the inelastic phase, the steel frame with the embedded SMA bracing system recovers the original shape because of the superelasticity. However, the steel frame with BRBF does not return to the initial state. This feature is the main advantage of the SMA-based system.

In order to study the re-centering ability of the SMA bracing system and the BRBF, the residual drifts of each story of the steel frame are computed. It is found that the residual drifts of each story of steel frame with the SMA-based device are remarkably lower than steel frame with the BRBF, as illustrated in Figure 12. Again, the superelasticity of the SMA plays a key role in this structural behaviour.

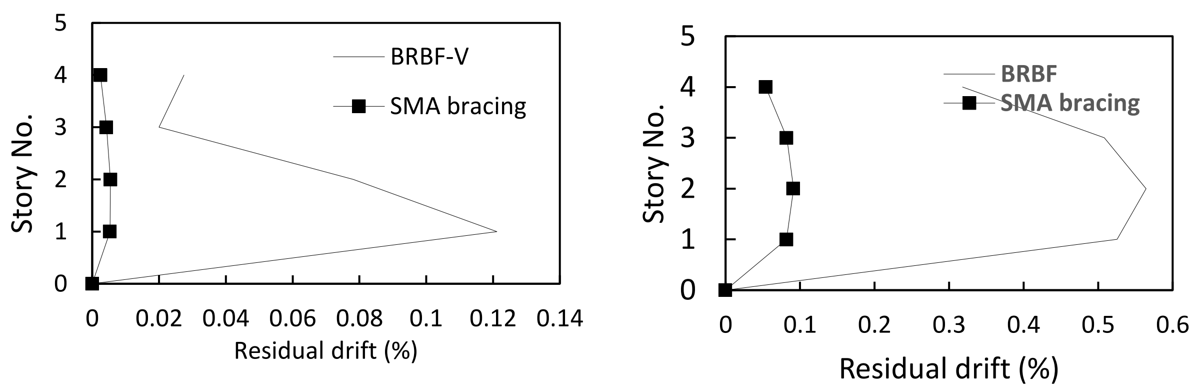

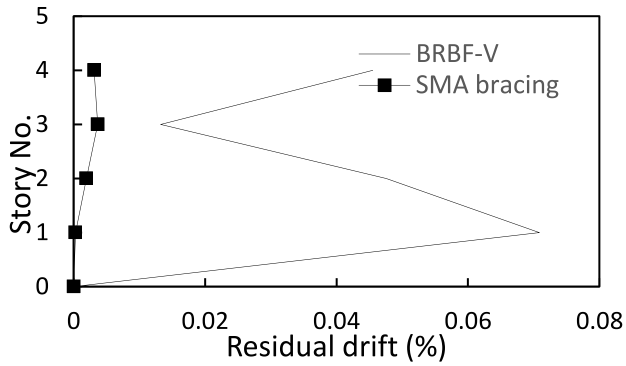

Figure 12. The residual drifts of the SMA bracing system and the BRBF under three ground motions

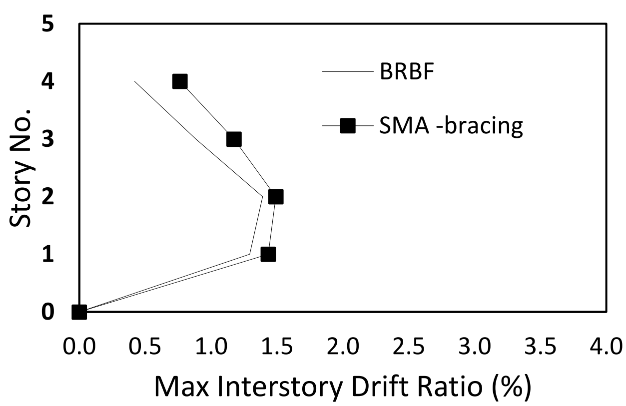

Figure 13 shows the maximum interstory drifts of the steel frame equipped with both bracing systems. As shown, in both cases the maximum interstory drift ratio is within the allowable range which is less than 2.5% based on Code 2014.

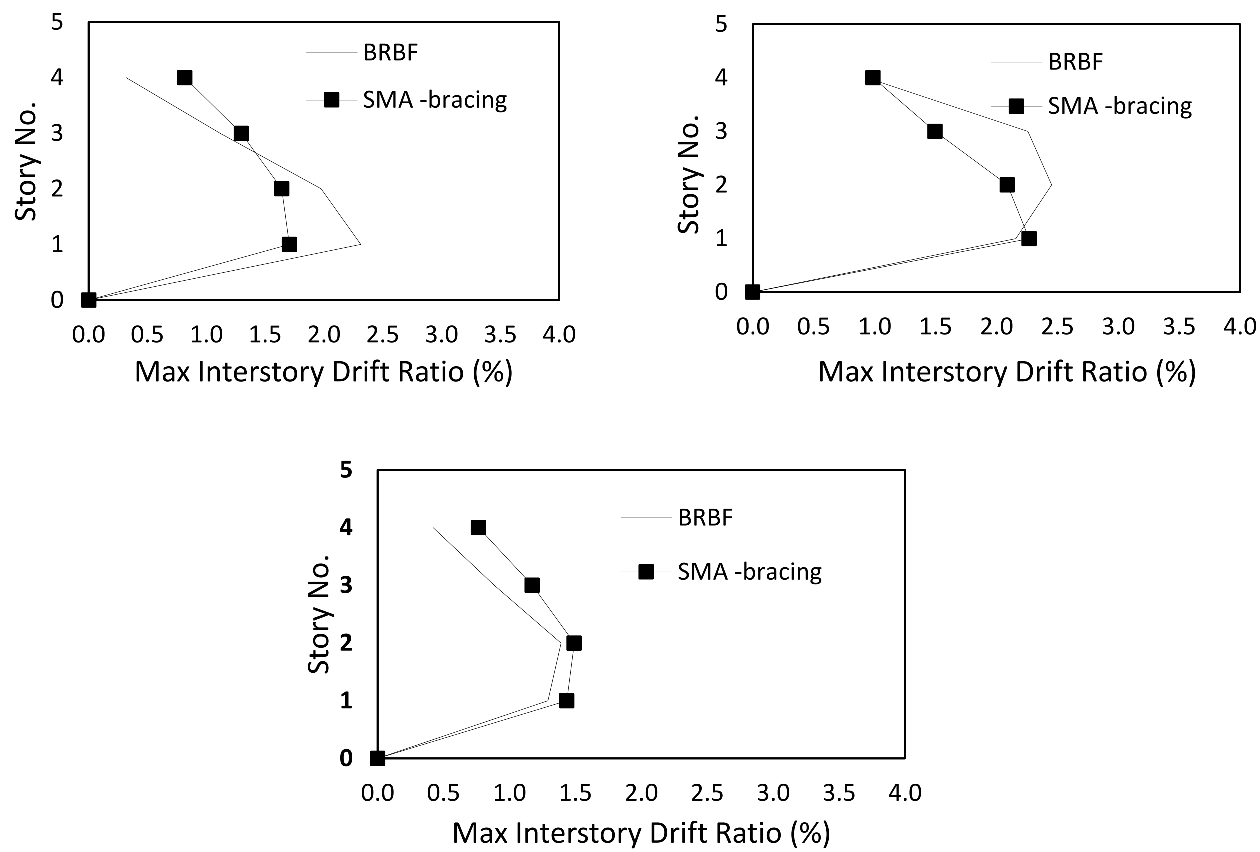

Figure 13. The maximum interstory drifts of the SMA bracing system and BRBF under three ground motions

1.9 Conclusion

In this study, the novel SMA bracing system is proposed to be integrated with the steel frame. In order to study the effect of the suggested system on structural response, the steel frames with the SMA bracing system and the BRBF are subjected to the three GMs. The main outcomes of study are as follows:

1. The major advantage of the suggested system compared to conventional bracing systems such as the BRBF is the re-centering ability. This re-centering ability is displayed in the residual drifts of the stories and the hysteresis response of the second story of the steel frame. The steel frame recovered its original shape with the SMAs system; the BRBF did not.
2. The amount of energy dissipation of the BRBF is greater than the SMA-based system. It is explained that the yield stress of steel is smaller than the Martensite start stress of the NiTi.

In future work, it is recommended that various SMA materials be used for the SMA bracing system and/or other types of dampers, such a friction damper, be added to the SMA bracing system in order to increase energy dissipation of civil infrastructure.

Acknowledgements

The authors wish to thank the support provided by the University of British Columbia Okanagan and the University of Tehran.

References

Code, I.S., 2014. Iranian code of practice for seismic resistant design of buildings 2800 (2014).

Dezfuli, F.H. & Alam, M.S., 2013. Shape memory alloy wire-based smart natural rubber bearing. *Smart Materials and Structures*, 22(4), pp.13–45.

Eatherton, M.R., Fahnestock, L.A. & Miller, D.J., 2014. Computational study of self-centering buckling-restrained braced frame seismic performance. *Earthquake Engineering & Structural Dynamics*, 43(13), pp.1897–1914.

Gao, N. et al., 2016. An innovative seismic bracing system based on a superelastic shape memory alloy ring. *Smart Materials and Structures*, 25(5), p.55030.

Hedayati Dezfuli, F., 2015. Hysteretic behaviour of steel-and fibre-reinforced elastomeric isolators fitted with superelastic shape memory alloy wire.

Hedayati Dezfuli, F. & Alam, M.S., 2013. Shape memory alloy wire-based smart natural rubber bearing. *Smart Materials and Structures*, 22(4), p.45013. Available at: http://stacks.iop.org/0964-1726/22/i=4/a=045013.

Krumme, R., Hayes, J. & Sweeney, S., 1995. Structural damping with shape-memory alloys: one class of devices. In *Smart Structures & Materials' 95*. pp. 225–240.

Massah, S.R. & Dorvar, H., 2014. Design and analysis of eccentrically braced steel frames with vertical links using shape memory alloys. *Smart Materials And Structures*, 23(11).

Moradi, S., Alam, M.S. & Asgarian, B., 2014. Incremental dynamic analysis of steel frames equipped with NiTi shape memory alloy braces. *The Structural Design of Tall and Special Buildings*, 23(18), pp.1406–1425.

Saber Moradi , M. Shahria Alam, B.A., 2014. Incremental dynamic analysis of steel frames equipped with NiTi shape memory alloy braces. *The Structural Design of Tall and Special Buildings*, 24(July 2014), pp.421–439.

Talebi, E., Tahir, M. M., Zahmatkesh, F., & Kueh, A. B, 2014. Comparative study on the behaviour of Buckling Restrained Braced frames at fire. *Journal of Constructional Steel Research*, 102, pp.1–12.

Talebi, E., & Zahmatkesh, 2010. Performance of BRBF System and Comparing it with the OCBF. *World Academy of Science, Engineering and Technology*, 4(8), pp.678–685.

Code, I.S., 2014. Iranian code of practice for seismic resistant design of buildings 2800 (2014).

Dezfuli, F.H. & Alam, M.S., 2013. Shape memory alloy wire-based smart natural rubber bearing. *Smart Materials and Structures*, 22(4), pp.13–45.

Eatherton, M.R., Fahnestock, L.A. & Miller, D.J., 2014. Computational study of self-centering buckling-restrained braced frame seismic performance. *Earthquake Engineering & Structural Dynamics*, 43(13), pp.1897–1914.

Gao, N., Jeon, J. S., Hodgson, D. E., & DesRoches, R. 2016. An innovative seismic bracing system based on a superelastic shape memory alloy ring. *Smart Materials and Structures*, 25(5), p.55030.

Hedayati Dezfuli, F., 2015. Hysteretic behaviour of steel-and fibre-reinforced elastomeric isolators fitted with superelastic shape memory alloy wire.

Hedayati Dezfuli, F. & Alam, M.S., 2013. Shape memory alloy wire-based smart natural rubber bearing. *Smart Materials and Structures*, 22(4), p.45013. Available at: http://stacks.iop.org/0964-

1726/22/i=4/a=045013.

Krumme, R., Hayes, J. & Sweeney, S., 1995. Structural damping with shape-memory alloys: one class of devices. In *Smart Structures & Materials' 95*. pp. 225–240.

Massah, S.R. & Dorvar, H., 2014. Design and analysis of eccentrically braced steel frames with vertical links using shape memory alloys. *Smart Materials And Structures*, 23(11).

Moradi, S., Alam, M.S. & Asgarian, B., 2014. Incremental dynamic analysis of steel frames equipped with NiTi shape memory alloy braces. *The Structural Design of Tall and Special Buildings*, 23(18), pp.1406–1425.

Saber Moradi , M. Shahria Alam, B.A., 2014. Incremental dynamic analysis of steel frames equipped with NiTi shape memory alloy braces. *The Structural Design of Tall and Special Buildings*, 24(July 2014), pp.421–439.

Talebi, E. et al., 2014. Comparative study on the behaviour of Buckling Restrained Braced frames at fire. *Journal of Constructional Steel Research*, 102, pp.1–12.

Talebi E, Tahir MM, Zahmatkesh F, K.A., 2010. Performance of BRBF System and Comparing it with the OCBF. *World Academy of Science, Engineering and Technology*, 4(8), pp.678–685.